Journal of Computational Electronics (2021) 20:2522–2529
https://doi.org/10.1007/s10825-021-01787-4

Using plasmonic cloaking method on infinite cylindrical structures and its applications

Afsaneh Rezaei[1] · **Farzad Mohajeri**[1] · **Zahra Hamzavi-Zarghani**[1]

Received: 13 November 2020 / Accepted: 16 September 2021 / Published online: 9 October 2021

Abstract
In recent years, cloaking using materials with negative electric permittivity or magnetic permeability has been studied and researched. It has been demonstrated that covering an object with a cloak having an electric permittivity or magnetic permeability that is negative or less than unity can cause a reduction of the scattering cross-section (SCS) of the object. In this paper, we solve the scattering problem for an object with a single- or multilayer cylindrical cloak and thus obtain the fundamental equations necessary to design such cloaks under two conditions, viz. with and without consideration of the effects of coupling when solving the scattering problem. Using the obtained equations we demonstrate that this technique can indeed reduce the visibility of the object.

Keywords Plasmonic · Metamaterial · Plasmonic cloak · Reverse polarization

1 Introduction

Humans have long been interested in becoming invisible, as found in stories from different nations. This human ambition has not been abandoned over the centuries. Nowadays, cloaking is no longer an unreachable dream as a result of the advancement of science. Researchers have looked for an answer to the question of whether a cloaking layer can be achieved to make an object invisible, at least in a limited frequency range. In 1961, Dolin investigated anisotropic nonhomogeneous structures and showed that they enabled an electromagnetic wave to pass through an object without perturbation [1]. Other structures were introduced by Pendry in 2006 [2] and Greenleaf in 2009 [3]. Also, Kerker published a paper entitled "Cloaked Objects" in 1975, which inspired Engheta and Alú to investigate invisibility based on the scattering cancellation method [4]. The advent of metamaterials and the advancement of fabrication technology for such artificial materials with extraordinary electromagnetic properties opened a new avenue for the achievement of cloaking, and many researchers have been attracted to the use of metamaterials for this purpose.

An electromagnetic cloaking layer is a device that can make an object that is exposed to electromagnetic waves become invisible in a given frequency range. In physics, cloaking means that the cloaked object does not produce any changes in the fields around it. In other words, a cloaked object does not produce reflected waves towards the source or scattered waves in other directions. Moreover, it does not absorb waves. In electromagnetic wave scattering theory, invisibility is the same as achieving a near-zero or ideally exactly zero SCS. Since the SCS is defined as the ratio of the scattered power density from the object to the incident power density, zero SCS means invisibility.

Several methods to achieve invisibility have been introduced to date, each offering some advantages and disadvantages. Some of the most famous methods are the coordinate transformation technique [5], transmission line techniques [6, 7], parallel-plates cloaking [8], the hybrid method [9], and active schemes [10]. Since anisotropic and inhomogeneous materials are used in the majority of these methods, the realization of a cloaking layer has been impossible in practice. However, this all changed with the introduction of plasmonic cloaking and the feasibility of fabricating such

✉ Farzad Mohajeri
mohajeri@shirazu.ac.ir

Afsaneh Rezaei
mohammad.fendereski@gmail.com

Zahra Hamzavi-Zarghani
zahrahamzavi@yahoo.com

[1] Department of Communications and Electronics, School of Electrical and Computer Engineering, Shiraz University, Shiraz, Iran

cloaking layers. In 2005, Engheta and Alú presented a new technique in their paper entitled "Achieving Transparency with Plasmonic and Metamaterial Coatings," which is realizable in practice through the use of isotropic and homogeneous materials [11]. In this method, which is based on the scattering cancellation method and is called "plasmonic cloaking," invisibility is obtained by using materials with an electric permittivity or magnetic permeability that is less than unity or negative. For instance, some metals near their plasma frequencies or metamaterials with negative parameters can be used [12]. It is worth noting that this idea of using layers with near-zero electric permittivity to achieve invisibility in quasistatic conditions has been introduced before for very small spheres (with a radius much smaller than the wavelength) [13]. However, in the method known as plasmonic cloaking, the scattering problem can be solved for more general cases (dynamic and nonstatic).

The main idea behind the achievement of invisibility using a plasmonic cloak is a significant reduction of the SCS of the combination of the object and cloaking layer. It is known that, the larger the size of an object, the larger its SCS. Therefore, it is expected that the SCS will increase when adding a plasmonic layer to an object. However, in the plasmonic cloaking method, the SCS is reduced by adding a properly designed layer with a negative or near-zero electric permittivity or magnetic permeability. Therefore, by optimizing the design of the cloaking layer parameters, the SCS of the combination can reach zero, resulting in invisibility.

A physical justification of the plasmonic cloaking operation can be presented as follows: According to Fig. 1, consider a spherical object with a dielectric constant of $\varepsilon_1 > \varepsilon_0$, covered by a layer with a dielectric constant of $\varepsilon_2 < \varepsilon_0$ which is illuminated by an electromagnetic wave.

Plasmonic cloaking offers several advantages compared with previous methods, such as its nonresonant nature, wider bandwidth [14], the robustness of the layer, i.e., that a small change in the geometry or frequency will not degrade the cloaking effect [15], obtaining transparency in both the near and far field for one or various particles [16], the penetration of the field into the object, and the lack of isolation from the environment, which allows the cloaked object to be used in measurement sensors [17].

In 2013, Farhat and colleagues presented a paper describing the possibility of achieving a controllable cloaking layer using graphene. They showed that, by biasing the graphene layers using an external direct-current (DC) voltage, it is possible to obtain a tunable cloaking layer for operation at different frequencies [18]. Another advantage of using graphene in the plasmonic cloaking technique is its easy realization in practice.

So far, most research has focused on achieving invisibility for spherical objects, while less work has been done on cylindrical structures [19]. This paper tries to address the issue of invisibility for infinite cylindrical structures.

2 Infinite cylindrical structures with a multilayer cloak

Engheta and Alú introduced a two-layer plasmonic cloak to achieve invisibility at some different frequencies [14]. Our goal is to investigate the scattering problem of a multilayer plasmonic cloak for cylindrical structures under plane-wave excitation. We first consider the desired number of layers and obtain the scattering coefficients in the general case. It is worth noting that the use of a multilayer cloak can result in a multifrequency effect as well as reduced scattering coefficients at higher harmonics, because the addition of each layer to the structure leads to an increase in the degrees of freedom in the design procedure, thus enabling the higher harmonics to be minimized simultaneously. Figure 2 shows a cross-section of such a multilayer cloak to make a cylindrical structure invisible.

The number of cloaking layers is $N-1$, and their axis is along the z direction. The radius of the considered invisible cylinder is a, while its electric permittivity and magnetic permeability are ε and μ, respectively. The radius of the rth cylinder is a_{cr}, while its electric permittivity and magnetic permeability are ε_{cr} and μ_{cr}, respectively.

This problem can be solved for either transverse electrical (TE) or transverse magnetic (TM) polarization. We continue

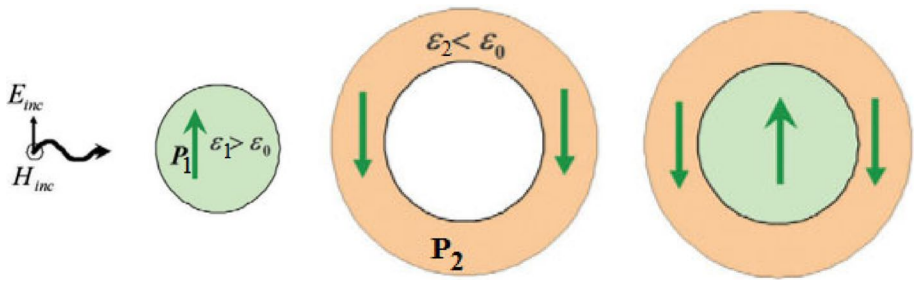

Fig. 1 **a** A spherical object with a dielectric constant of more than 1. **b** A spherical object covered by a layer with a dielectric constant of less than 1. **c** The cancellation of the polarization vectors of the object and layer results in a significant reduction of their SCS

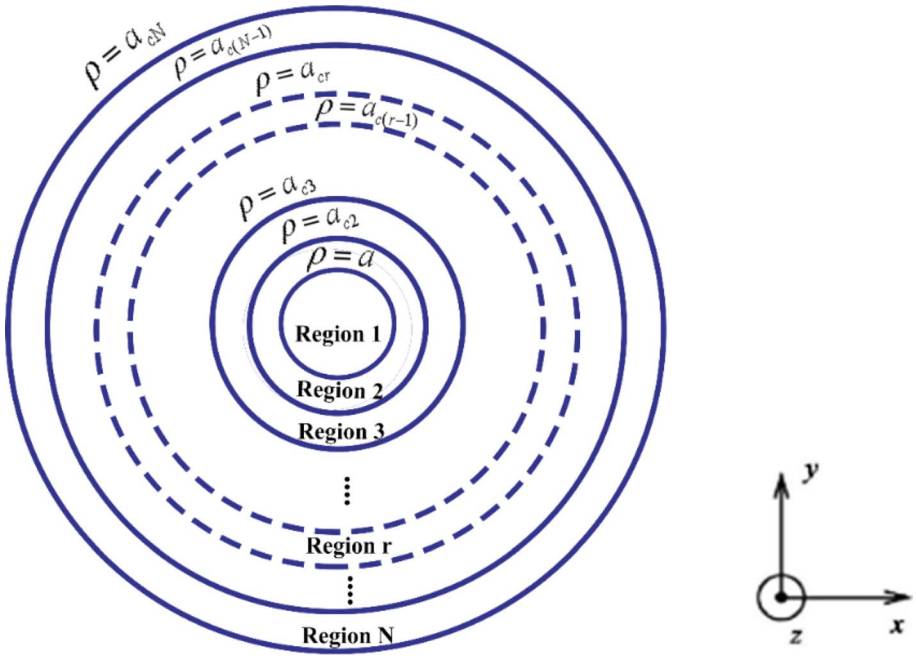

Fig. 2 A cross-section of a multilayer cloak for an infinite cylinder

our investigation by considering scattering of TM polarization by such cylinders, as this effect is much higher than for TE polarization.

Consider a TM$_z$-polarized plane wave with time dependence of $e^{-j\omega t}$ incident on the structure shown in Fig. 2. The incident wavevector can be written in the form of Eq. (1) [20].

$$\boldsymbol{E^i} = E_0 \hat{a}_z e^{-jk_0 x}, \tag{1}$$

where $k_0 = \omega\sqrt{\varepsilon_0 \mu_0}$ is the wavenumber in air.

By transforming from Cartesian to cylindrical coordinates, the tangential incident electric field can be written in the form of Eq. (2) [20].

$$E_z^i = E_0 \sum_{-\infty}^{+\infty} j^{-n} J_n(k_0\rho) e^{jn\varphi}. \tag{2}$$

The total tangential electric field in air consists of two parts, corresponding to the incident wave and the scattered wave. The electric field of the scattered wave in the z direction can be written according to Eq. (3).

$$E_z^{\text{scat}} = E_0 \sum_{-\infty}^{+\infty} C_{s,n}^{\text{TM}} j^{-n} H_n^{(2)}(k_0\rho) e^{jn\varphi}, \tag{3}$$

where $H_n^{(2)}$ is the Hankel function of the second kind. For the special case of normal incidence, the electric field in all the layers can be written as

$$\begin{aligned}
E_z^1 &= E_0 \sum_{-\infty}^{+\infty} j^{-n} C_{1,n}^{\text{TM}} J_n(k\rho) e^{jn\varphi},\\
E_z^2 &= E_0 \sum_{-\infty}^{+\infty} j^{-n} [C_{2i,n}^{\text{TM}} J_n(k_{c2}\rho) + C_{2o,n}^{\text{TM}} Y_n(k_{c2}\rho)] e^{jn\varphi},\\
E_z^3 &= E_0 \sum_{-\infty}^{+\infty} j^{-n} [C_{3i,n}^{\text{TM}} J_n(k_{c3}\rho) + C_{3o,n}^{\text{TM}} Y_n(k_{c3}\rho)] e^{jn\varphi},\\
&\vdots\\
E_z^r &= E_0 \sum_{-\infty}^{+\infty} j^{-n} [C_{ri,n}^{\text{TM}} J_n(k_{cr}\rho) + C_{ro,n}^{\text{TM}} Y_n(k_{cr}\rho)] e^{jn\varphi},\\
&\vdots\\
E_z^N &= E_0 \sum_{-\infty}^{+\infty} j^{-n} [C_{Ni,n}^{\text{TM}} J_n(k_{cN}\rho) + C_{No,n}^{\text{TM}} Y_n(k_{cN}\rho)] e^{jn\varphi},
\end{aligned} \tag{4}$$

where J_n and Y_n are Bessel functions of the first and second kind, respectively, $C_{s,n}^{\text{TM}}$ are scattering coefficients, $k = \omega\sqrt{\mu\varepsilon}$ and $k_{cr} = \omega\sqrt{\mu_{cr}\varepsilon_{cr}}$ are the wavenumbers in the cylindrical layers.

It is worth noting that, because we neglect the mutual coupling, the magnetic field of the scattered wave in the z direction is zero: ($H_z^{\text{scat}} = 0$).

To obtain the unknown coefficients in Eq. (4), continuity of the tangential electric and magnetic fields should be applied at all the intersections. The tangential magnetic fields are calculated from Maxwell's equations as follows [20]:

$$H_{\varphi} = -\frac{1}{\mathrm{j}\omega\mu}\left[\frac{\partial}{\partial z}\left(-\frac{1}{\mathrm{j}\omega\varepsilon}\frac{\partial H\varphi}{\partial z}\right) - \frac{\partial E_z}{\partial \rho}\right]. \tag{5}$$

By applying the boundary conditions at the intersections $\rho = a, a_{c2}, a_{c3\ldots}\, a_{cN}$, the following $2N$ equations are obtained:

$$\begin{aligned}
&C^{\mathrm{TM}}_{2i,n}J_n(k_{c2}a) + C^{\mathrm{TM}}_{2o,n}Y_n(k_{c2}a) = C^{\mathrm{TM}}_{1,n}J_n(ka)\\
&C^{\mathrm{TM}}_{2i,n}J_n(k_{c2}a_{c2}) + C^{\mathrm{TM}}_{2o,n}Y_n(k_{c2}a_{c2}) = C^{\mathrm{TM}}_{3i,n}J_n(k_{c3}a_{c2}) + C^{\mathrm{TM}}_{3o,n}Y_n(k_{c3}a_{c2})\\
&C^{\mathrm{TM}}_{3i,n}J_n(k_{c3}a_{c3}) + C^{\mathrm{TM}}_{3o,n}Y_n(k_{c3}a_{c3}) = C^{\mathrm{TM}}_{4i,n}J_n(k_{c4}a_{c3}) + C^{\mathrm{TM}}_{4o,n}Y_n(k_{c4}a_{c3})\\
&\vdots\\
&C^{\mathrm{TM}}_{ri,n}J_n(k_{cr}a_{cr}) + C^{\mathrm{TM}}_{ro,n}Y_n(k_{cr}a_{cr}) = C^{\mathrm{TM}}_{(r+1)i,n}J_n(k_{c(r+1)}a_{cr}) + C^{\mathrm{TM}}_{(r+1)o,n}Y_n(k_{c(r+1)}a_{cr})\\
&\vdots\\
&C^{\mathrm{TM}}_{Ni,n}J_n(k_{cN}a_{cN}) + C^{\mathrm{TM}}_{No,n}Y_n(k_{cN}a_{cN}) = J_n(k_0a_{cN}) + C^{\mathrm{TM}}_{s,n}H^{(2)}_n(k_0a_{cN})
\end{aligned} \tag{6}$$

$$\begin{aligned}
&\frac{1}{\eta_{c2}}C^{\mathrm{TM}}_{2i,n}J'_n(k_{c2}a) + \frac{1}{\eta_{c2}}C^{\mathrm{TM}}_{2o,n}Y'_n(k_{c2}a) = \frac{1}{\eta}C^{\mathrm{TM}}_{1,n}J'_n(ka)\\
&\frac{1}{\eta_{c2}}C^{\mathrm{TM}}_{2i,n}J'_n(k_{c2}a_{c2}) + \frac{1}{\eta_{c2}}C^{\mathrm{TM}}_{2o,n}Y'_n(k_{c2}a_{c2}) = \frac{1}{\eta_{c3}}C^{\mathrm{TM}}_{3i,n}J'_n(k_{c3}a_{c2}) + \frac{1}{\eta_{c3}}C^{\mathrm{TM}}_{3o,n}Y'_n(k_{c3}a_{c2})\\
&\frac{1}{\eta_{c3}}C^{\mathrm{TM}}_{3i,n}J'_n(k_{c3}a_{c3}) + \frac{1}{\eta_{c3}}C^{\mathrm{TM}}_{3o,n}Y'_n(k_{c3}a_{c3}) = \frac{1}{\eta_{c4}}C^{\mathrm{TM}}_{4i,n}J'_n(k_{c4}a_{c3}) + \frac{1}{\eta_{c4}}C^{\mathrm{TM}}_{4o,n}Y'_n(k_{c4}a_{c3})\\
&\vdots\\
&\frac{1}{\eta_{cr}}C^{TM}_{ri,n}J'_n(k_{cr}a_{cr}) + \frac{1}{\eta_{cr}}C^{TM}_{ro,n}Y'_n(k_{cr}a_{cr}) = \frac{1}{\eta_{c(r+1)}}C^{TM}_{(r+1)i,n}J'_n(k_{c(r+1)}a_{cr}) + \frac{1}{\eta_{c(r+1)}}C^{TM}_{(r+1)o,n}Y'_n(k_{c(r+1)}a_{cr})\\
&\vdots\\
&\frac{1}{\eta_{cN}}C^{TM}_{Ni,n}J'_n(k_{cN}a_{cN}) + \frac{1}{\eta_{cN}}C^{TM}_{No,n}Y'_n(k_{cN}a_{cN}) = \frac{1}{\eta_0}J'_n(k_0a_{cN}) + \frac{1}{\eta_0}C^{TM}_{s,n}H'^{(2)}_n(k_0a_{cN}),
\end{aligned}$$

where $J_n{}'$ and $Y_n{}'$ are the derivative of Bessel functions of the first and second kind, respectively, $H'^{(2)}_n$ is the derivative of the Hankel function of the second kind with respect to the argument, and $\eta = \sqrt{\frac{\mu}{\varepsilon}}$ and $\eta_{cr} = \sqrt{\frac{\mu_{cr}}{\varepsilon_{cr}}}$ are the intrinsic impedances in the layers. Equations (6) form a system of linear and inhomogeneous equations with $2N$ unknown coefficients. By solving these equations, the scattering coefficients are obtained as

$$C^{\mathrm{TM}}_{s,n} = \frac{|\Delta'|}{|\Delta|} \tag{7}$$

where

$$\Delta = \begin{bmatrix} A_1\\ A_2\\ A_3\\ \vdots\\ A_r\\ \vdots\\ A_{N-1}\\ A_N \end{bmatrix} \tag{8}$$

And

$$\Delta' = \begin{bmatrix} A_1\\ A_2\\ A_3\\ \vdots\\ A_r\\ \vdots\\ A_{N-1}\\ B_N \end{bmatrix}, \tag{9}$$

where the coefficients $A_1, A_2, \ldots, A_r, \ldots, A_N$ and B_N are $2 \times 2N$ matrices that are evaluated as follows:

$$A_1 = \begin{bmatrix} -J_n(ka) & J_n(k_{c2}a) & Y_n(k_{c2}a) & 0 & 0 \dots 0 \\ -\frac{1}{\eta}J'_n(ka) & \frac{1}{\eta_{c2}}J'_n(k_{c2}a) & \frac{1}{\eta_{c2}}Y'_n(k_{c2}a) & 0 & 0 \dots 0 \end{bmatrix}$$

$$A_2 = \begin{bmatrix} 0 & J_n(k_{c2}a_{c2}) & Y_n(k_{c2}a_{c2}) & -J_n(k_{c3}a_{c2}) - Y_n(k_{c3}a_{c2}) & 0 \dots 0 \\ 0 & \frac{1}{\eta_{c2}}J'_n(k_{c2}a_{c2}) & \frac{1}{\eta_{c2}}Y'_n(k_{c2}a_{c2}) - \frac{1}{\eta_{c3}}J'_n(k_{c3}a_{c2}) & -\frac{1}{\eta_{c3}}Y'_n(k_{c3}a_{c2}) & 0 \dots 0 \end{bmatrix}$$

$$A_3 = \begin{bmatrix} 00 & J_n(k_{c3}a_{c3}) & Y_n(k_{c3}a_{c3}) & -J_n(k_{c4}a_{c3}) - Y_n(k_{c4}a_{c3}) & 0 \dots 0 \\ 00 & \frac{1}{\eta_{c3}}J'_n(k_{c3}a_{c3}) & \frac{1}{\eta_{c3}}Y'_n(k_{c3}a_{c3}) - \frac{1}{\eta_{c4}}J'_n(k_{c4}a_{c3}) & -\frac{1}{\eta_{c4}}Y'_n(k_{c4}a_{c3}) & 0 \dots 0 \end{bmatrix}$$

$$\vdots$$

$$A_r = \begin{bmatrix} 0 \dots 0 & J_n(k_{cr}a_{cr}) & Y_n(k_{cr}a_{cr}) & -J_n(k_{c(r+1)}a_{cr}) - Y_n(k_{c(r+1)}a_{cr}) & 0 \dots 0 \\ 0 \dots 0 & \frac{1}{\eta_{cr}}J'_n(k_{cr}a_{cr}) & \frac{1}{\eta_{cr}}Y'_n(k_{cr}a_{cr}) - \frac{1}{\eta_{c(r+1)}}J'_n(k_{c(r+1)}a_{cr}) & -\frac{1}{\eta_{c(r+1)}}Y'_n(k_{c(r+1)}a_{cr}) & 0 \dots 0 \end{bmatrix} \tag{10}$$

$$\vdots$$

$$A_{N-1} = \begin{bmatrix} 0 \dots 0 & J_n(k_{c(N-1)}a_{c(N-1)}) & Y_n(k_{c(N-1)}a_{c(N-1)}) & -J_n(k_{cN}a_{cN}) - Y_n(k_{cN}a_{cN}) & 0 \\ 0 \dots 0 & \frac{1}{\eta_{c(N-1)}}J'_n(k_{c(N-1)}a_{c(N-1)}) & \frac{1}{\eta_{c(N-1)}}Y'_n(k_{c(N-1)}a_{c(N-1)}) - \frac{1}{\eta_{cN}}J'_n(k_{cN}a_{cN}) & -\frac{1}{\eta_{cN}}Y'_n(k_{cN}a_{cN}) & 0 \end{bmatrix}$$

$$A_N = \begin{bmatrix} 0 & 0 \dots 0 & J_n(k_{cN}a_{cN}) & Y_n(k_{cN}a_{cN}) & -H_n^{(2)}(k_0a_{cN}) \\ 0 & 0 \dots 0 & \frac{1}{\eta_{cN}}J'_n(k_{cN}a_{cN}) & \frac{1}{\eta_{cN}}Y'_n(k_{cN}a_{cN}) & -\frac{1}{\eta_0}H'^{(2)}_n(k_0a_{cN}) \end{bmatrix}$$

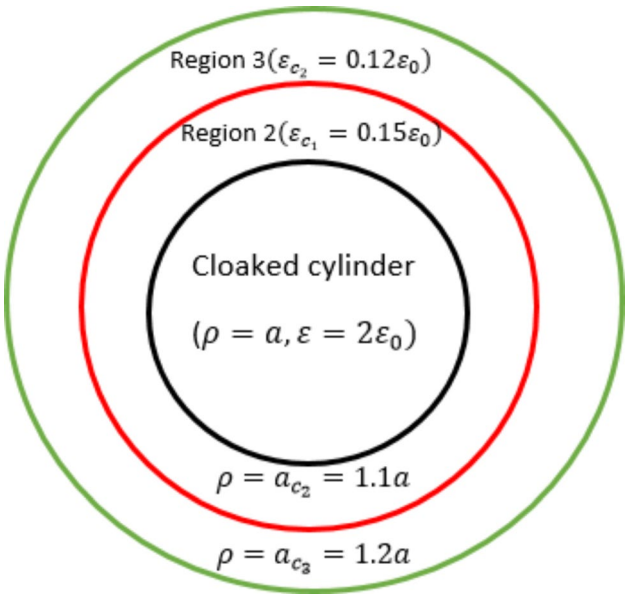

Fig. 3 A dielectric cylinder covered by two cloaking layers

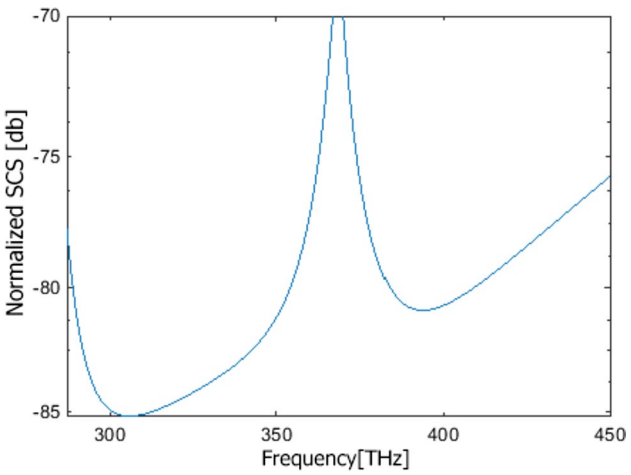

Fig. 4 The normalized SCS of a dielectric cylinder with radius of 10 nm covered by two plasmonic layers

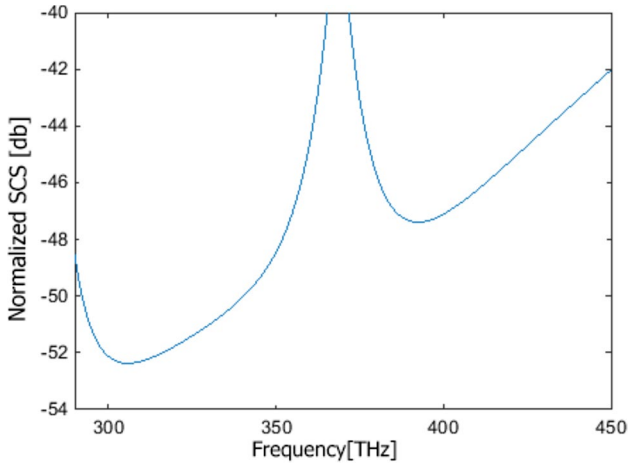

Fig. 5 The normalized SCS of a dielectric cylinder with radius of 30 nm covered by two plasmonic layers

$$B_N = \begin{bmatrix} 0 & 0 \dots & 0 & J_n(k_{cN}a_{cN}) & Y_n(k_{cN}a_{cN}) & J_n(k_0 a_{cN}) \\ 0 & 0 \dots & 0 & \frac{1}{\eta_{cN}} J_n'(k_{cN}a_{cN}) & \frac{1}{\eta_{cN}} Y_n'(k_{cN}a_{cN}) & \frac{1}{\eta_0} J_n'(k_0 a_{cN}) \end{bmatrix}.$$

3 Simulation results

In this section, simulation results for a dielectric cylinder covered by two cloaking layers as shown in Fig. 3 are described.

Figures 4 and 5 show the normalized scattering cross-section (SCS) of the cloaked cylinder for two values of the radius, viz. $a = 10$ nm and $a = 30$ nm, respectively, with a dielectric constant of 2. Also $a_{c2} = 1.1a$ and $a_{c3} = 1.2a$ are the radii of the first and second covering layer. The values of the electric permittivity coefficients for these layers, obtained by using the Drude model at the desired frequencies, are $\varepsilon_{c1} = 0.15\varepsilon_0$ and $\varepsilon_{c2} = 0.12\varepsilon_0$. Also the losses of the two layers lie in the acceptable range according to the Drude model.

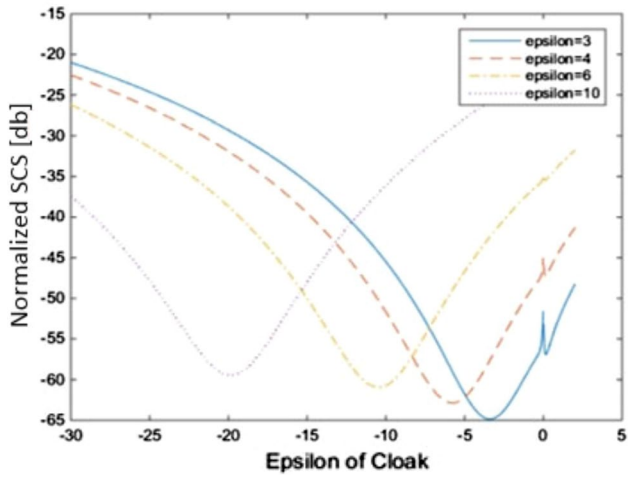

Fig. 6 The normalized SCS of a dielectric cylinder with radius of 100 nm with respect to the relative electric permittivity of the first cloak for different electric permittivity values of the central cylinder

It can be concluded that, by using two cloaking layers, invisibility is obtained at two frequencies. It is also observed that trhe reduction in the scattering decreases at higher frequencies as a result of the increasing $k_0 a$ and because the object becomes electrically larger. Therefore, increasing the higher harmonics of thescattering coefficients leads to a reduction of the cloaking performance, which is in complete accordance with the findings in Ref. [11] for spherical cloaks.

To better understand the performance of such a plasmonic cloak, it is worth examining the behavior of the normalized SCS of the central cylinder with respect to the relative electric permittivity of region 2 in Fig. 3 by changing its electric permittivity (Fig. 6).

In this case, the radius of the central cylinder is chosen as $a = 100$ nm, the radii of the plasmonic cloaking layers are $a_{c2} = 1.1a$ and $a_{c3} = 1.2a$, $k_0 a = 0.1$ rad, and the relative electric permittivity of the cloaked cylinder is chosen as 3, 4, 6, or 10.

As can be seen, for a cylinder with a higher electric permittivity, cloaks with a more negative electric permittivity are needed. As a result, the cloaking performance is clearly degraded. The reason for this is that, with increasing electric permittivity of the cylinder, the scattering coefficients become larger and thus invisibility becomes more difficult to achieve. Therefore, the performance of the plasmonic cloak also decreases.

At this point, it is appropriate to examine the performance of the cylindrical cloak in relation to changes in the radius of the central cylinder in Fig. 3. Figure 7 shows the values of the normalized SCS in terms of the relative electric permittivity of region 2 for radii of the central cylinder of $a = 10$, 50, 100, and 500 nm at a frequency of 100 THz.

As can be seen, the normalized SCS decreases sharply for certain values of the relative electric permittivity of the cloak, and this occurs for all radii of the central cylinder. These values of the relative electric permittivity of the cloak are all negative. It is thus possible to minimize the scattering coefficients in Eq. (6) by using plasmonic or metamaterial cloaks, thereby achieving transparency. It is also observed that the rate of drop of the normalized SCS decreases with increasing radius of the central cylinder. This phenomenon occurs due to the appearance of higher terms in the SCS relation, being consistent with the findings reported in Ref. [18] for the performance of spherical cloaks. Also, the location of the drop in the normalized SCS in Fig. 7a, b is almost the same for cylinders with small radii, but when increasing the radius of the cylinder in Fig. 7c, d, the values

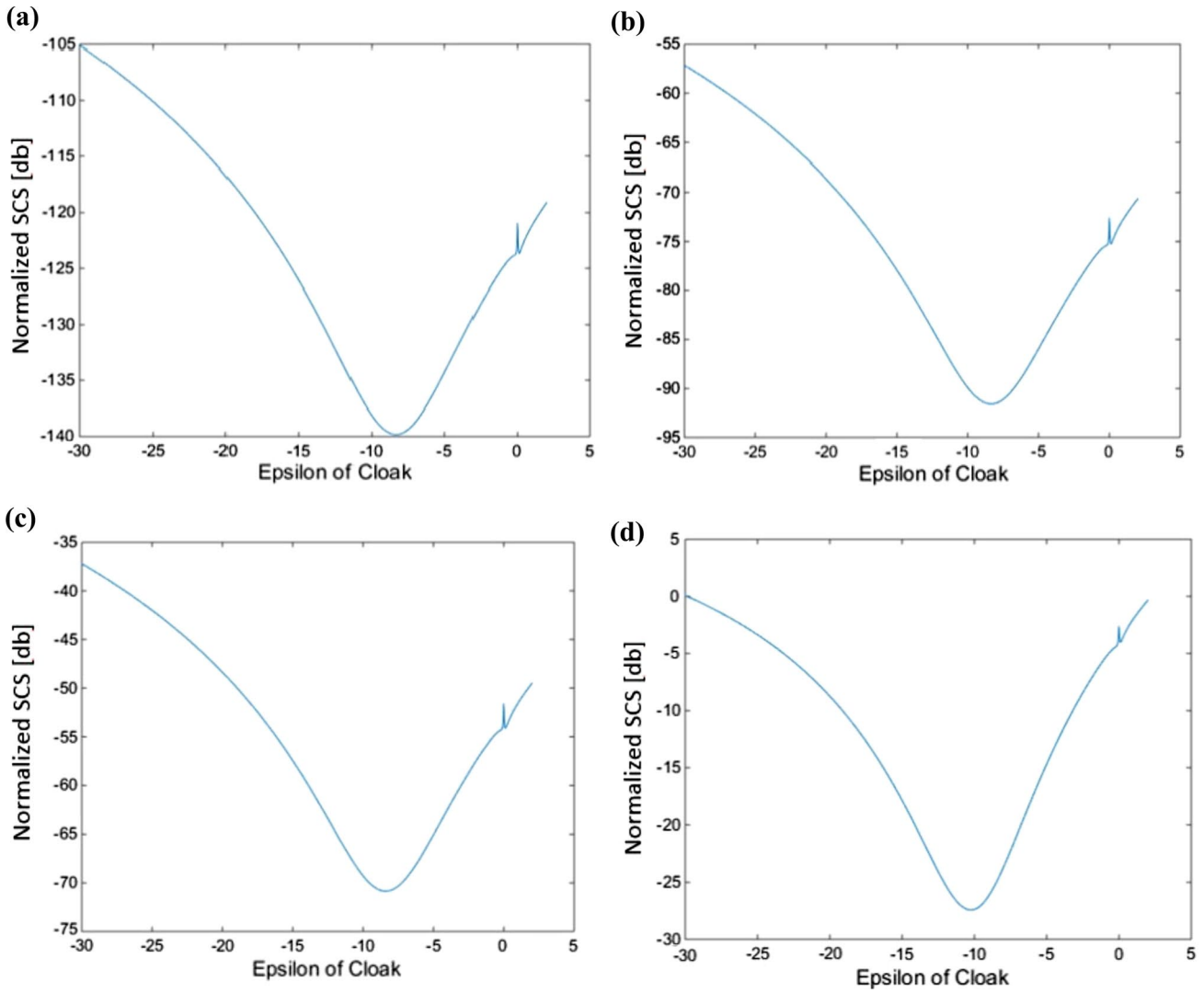

Fig. 7 The normalized SCS of a dielectric central cylinder with radius of **a** 10 nm, **b** 50 nm, **c** 100 nm, and **d** 500 nm, with respect to the relative electric permittivity of the first cloak

Table 1 A comparison of cloaking methods described in literature versus the current work

Ref.	Radius of the cylinder (λ)	RCS reduction (dB)	Cloaking method	Multilayer and multifrequency
[21]	0.1	10	Plasmonic cloaking	×
[22]	0.13	13	Mantle cloaking	×
[23]	0.13	8	Core–shell nanoparticles	×
[24]	0.12	12	Graphene metasurface	×
[25]	0.1	13.5	Graphene monolayer	×
[14]	0.2	10	Plasmonic cloaking	✓
This work	0.17	26	Plasmonic cloaking	✓

RCS radar cross section

of the relative electric permittivity of the cloak where the SCS drops change. The reason for this is that, for cylinders with a smaller radius, the Bessel functions in the scattering coefficient relations (Eq. 6), can be approximated by a small-argument approximation, and finally a closed form can be obtained to minimize the scattering coefficients. Since this

closed form is a function of the ratio of the radius of the cylinder to the radius of the cloak, and here this ratio is the same in all the designs in Fig. 7, it is almost the same for small cylinders, but with increasing radius of the cylinder, this approximation is not valid. The location where the SCS drops thus changes with the radius of the cylinder.

The main advantage of the cloaking structure proposed herein in comparison with other literature reports is that, in previous works, such multilayer cloaking structures were not studied analytically using precise mathematical equations, or this was done only for two-layer structures, while the current analysis of these structures is completely accurately and enjoys mathematical support. Obviously, this precise mathematical analysis could also be applied for the particular case of two-layer structures.

Table 1 compares different cloaking techniques. It shows that, considering the radius of the cylinder, the radar cross section (RCS) reduction, and whether they offer multilayer, multifrequency operation, the method presented herein offers good performance.

4 Conclusions

The use of metamaterial or plasmonic cloaks with a negative or near-zero relative electric permittivity to reduce the scattering from a structure by creating reverse polarization and thus invisibility is investigated herein.

A design procedure for the multilayer plasmonic cloak to achieve invisibility for an infinite dielectric cylinder is described. The resulting analysis is completely accurately and enjoys mathematical support. Simulation results for the SCS of cylinders cloaked using two plasmonic layers are presented, verifying the cloaking effect at two frequencies. The behavior of the normalized SCS of the central cylinder with respect to its radius and electric permittivity is also investigated.

References

1. Dolin, L.S.: To the possibility of comparison of three-dimensional electromagnetic systems with nonuniform anisotropic filling. Izvestiya Vuzov Radiofizika **4**(5), 964–967 (1961)
2. Pendry, J.B., Schurig, D., Smith, D.R.: Controlling electromagnetic fields. Science **312**, 1780–1782 (2006)
3. Greenleaf, A., Kurylev, Y., Lassas, M., Uhlmann, G.: Cloaking devices, electromagnetic wormholes, and transformation optics. SIAM Rev. **51**(1), 3–33 (2009)
4. Kerker, M.: Invisible bodies. J. Opt. Soc. Am. **65**(4), 376–379 (1975)
5. Alù, A., Bilotti, F., Vegni, L.: Method of lines numerical analysis of conformal antennas. IEEE Trans. Antennas Propag. **52**(6), 1530–1540 (2004)
6. Alitalo, P., Luukkonen, O., Jylha, L., Venermo, J., Tretyakov, S.A.: Transmission-line networks cloaking objects from electromagnetic fields. IEEE Trans. Antennas Propag. **56**(2), 416–424 (2008)
7. Alitalo, P., Ranvier, S., Vehmas, J., Tretyakov, S.: A microwave transmission-line network guiding electromagnetic fields through a dense array of metallic objects. Metamaterials **2**(4), 206–212 (2008)
8. Alitalo, P., Culhaoglu, A.E., Osipov, A.V., Thurner, S., Kemptner, E., Tretyakov, S.A.: Bistatic scattering characterization of a three-dimensional broadband cloaking structure. J. Appl. Phys. **111**(3), 034901–034905 (2012)
9. Nicorovici, N.A., Milton, G.W., McPhedran, R.C., Botten, L.C.: Quasistatic cloaking of two dimensional polarizable discrete systems by anomalous resonance. Opt. Express **15**(10), 6314–6323 (2007)
10. Nicorovici, N.P., McPhedran, R.V., Enoch, S., Tayeb, G.: Finite wavelength cloaking by plasmonic resonance. New J. Phys. **10**(11), 115020 (2008)
11. Alù, A., Engheta, N.: Achieving transparency with plasmonic and metamaterial coatings. Phys. Rev. E **72**(1), 016623 (2005)
12. Johnson, P.B., Christy, R.W.: Optical constants of the noble metals. Phys. Rev. B **6**(12), 4370–4379 (1972)
13. Chew, H., Kerker, M.: Abnormally low electromagnetic scattering cross sections. J. Opt. Soc. Am. **66**(5), 445 (1976)
14. Alù, A., Engheta, N.: Theory and potentials of multi-layered plasmonic covers for multi-frequency cloaking. New J. Phys. **10**, 115036 (2008)
15. Alù, A., Engheta, N.: Plasmonic materials in transparency and cloaking problems: mechanism, robustness, and physical insights. Opt. Express **15**(6), 3318–3332 (2007)
16. Alù, A., Engheta, N.: Cloaking and transparency for collections of particles with metamaterial and plasmonic covers. Opt. Express **15**(12), 7578–7590 (2007)
17. Alù, A., Engheta, N.: Cloaking a sensor. Phys. Rev. Lett. **102**, 233901 (2009)
18. Farhat, M., Rockstuhl, C., Bagci, H.: A 3D tunable and multi-frequency graphene plasmonic cloak. Opt. Express **21**(10), 12592–12603 (2013)
19. Alù, A., Rainwater, D., Kerkhoff, A.: Plasmonic cloaking of cylinders: finite length, oblique illumination and cross-polarization coupling. New J. Phys. **12**, 103028 (2010)
20. Balanis, C.A.: Advanced Engineering Electromagnetics. Wiley, New York (1989)
21. Bilotti, F., Tricarico, S., Vegni, L.: Electromagnetic cloaking devices for TE and TM polarizations. New J. Phys. **12**, 115035 (2008)
22. Danaeifar, M., Booket, M., Granpayeh, N.: Optical invisibility of cylindrical structures and homogeneity effect on scattering cancellation method. Electron. Lett. **52**, 29–31 (2016)
23. Monti, A., Bilotti, F., Toscano, A.: Optical cloaking of cylindrical objects by using covers made of core-shell nanoparticles. Opt. Lett. **36**, 4479–4481 (2011)
24. Chen, P.Y., et al.: Nanostructured graphene metasurface for tunable terahertz cloaking. New J. Phys. **15**, 123029 (2013)
25. Hamzavi-Zarghani, Z., Yahaghi, A., Matekovits, L.: Electrically tunable mantle cloaking utilizing graphene metasurface for oblique incidence. Int. J. Electron. Commun. **116**, 153080 (2020)